Reliability Oriented Modeling and Analysis of PLC for EVs to Charging Piles Communication System Based on IPA-SAMP Impulse Noise Cancelation

LIANG ZHANG[1], **(Member, IEEE), SHENGBIN CHI**[1], **QUANGUI HU**[2], **KANG CHEN**[1], **AND LING LYU**[1]
[1]School of Electrical Engineering, Northeast Electric Power University, Jilin 132012, China
[2]Sgitg Accenture Information Technology Center, Beijing 100031, China

Corresponding author: Liang Zhang (xiaozhanghit@163.com)

ABSTRACT With the development of new energy technology, the number of electric vehicles (EVs) will continue to increase, which will seriously threaten the safe operation of the power grid. The V2G information interaction system can help the power grid to achieve safe and reliable operation. Therefore, under the framework of the V2G information interaction system, this paper establishes the communication system between EVs and charging piles based on power line communication (PLC), which can reduce the cost and avoid the problem that the incompatible communication interface caused by different specifications of charging piles. Due to the severe impulse noise (IN) communication environments between EVs and charging piles, the transmission performance would be seriously degraded. Hence, an improved-priori-aided sparsity adaptive matching pursuit (IPA-SAMP) is proposed to reconstruct IN. In the process of IN cancelation, the measurement vector is obtained from the null sub-carriers. In order to efficiently reconstruct IN, as the input of the IPA-SAMP algorithm, partial support are improved by the optimized threshold, which significantly improve the accuracy and robustness of the recovered IN. The proposed IPA-SAMP algorithm can effectively recover IN in the channel between EVs and charging piles, improves the reliability of the information exchange system, which is validated by computer simulations.

INDEX TERMS V2G, power line communication (PLC), impulse noise (IN), improved priori-aided sparsity adaptive matching pursuit (IPA-SAMP), communication system between EVs and charging piles, reliability.

I. INTRODUCTION

EVs could reduce the fossil fuel consumption and emission rates, while the large scale EVs' charging demand also have a negative impact on power grid, which could give a severe impact on the power network, affecting the security of power grids, if EVs charging is not managed properly [1]. Aiming at the effect of EVs charging demand on the power network, a novel model to study the effects of power exchange between the grid and EVs was proposed in [2]. A two-stage approach for allocation of EV parking lots and distributed renewable resources (DRRs) in power distribution network was proposed to reduce the impact of EVs charging demand on the

power grid, and realize the sustainable development of power grid in an environmentally-friendly way [3]. Their model are based on EVs' energy flow.

Additionally, with the support of the latest status information of EVs, the impact caused by EVs' charging demand on the grid network could be greatly attenuated [4]. According to the International Energy Agency (IEA), the number of EVs in the globe will reach 13 million units by 2020 and nearly 130 million units by 2030, which makes it's urgent for us to establish a communication network to obtain EVs' status information. The V2G information interaction system could achieve information interaction between EVs and the grid, but there are still many challenges that need to be resolved before a stable communication system is developed [5].

The associate editor coordinating the review of this manuscript and approving it for publication was Cesar Vargas-Rosales.

In order to address the challenges, such as low reliability and cyberattacks, Authors in [6]–[11] proposed some solutions that to ensure the information exchange between EVs and the charging stations. In this paper, we mainly solve the problem of information exchange between EVs and charging piles.

The communication system between EVs and charging piles requires high reliability and low latency [12]. CAN and wireless communication are the traditional solution to realize the high reliability and low latency communication [13], [14], while CAN communication need to lay the communication line in the charging cables and wireless communication require the installation of wireless communication infrastructure on charging piles' and EVs' side, which makes it's uneconomical and more complicated. Furthermore, in our previously work, the structure of a V2G information exchange system based on PLC was proposed and we have demonstrated the reliability about the vehicular power line communication (VPLC) [5]. In this paper, PLC is continued to adopt to realize the communication between EVs and charging piles, which could simplify the charging interface and the charging line, reduce the cost and don't need the communication protocol conversion.

The channel attenuation and IN are the two main factors affect the reliability between EVs and charging piles based on PLC. However, due to the presence of the sensors, electronic devices, converters and other electronic devices in EVs and charging piles, the impact of IN are severe, which affects the accuracy of the information.

To mitigate IN, some traditional methods have been proposed. In [15], the clipping and/or blanking method were proposed to produce nonlinear processors for receivers against IN. Since the effect of IN with high intensity cannot be effectively eliminated by traditional methods through suppressing the power of IN or clipping/blanking the useful data, which might cause data loss and performance degradation [16]. In order to accurately realize the recovery of IN, compressed sensing (CS) is introduced by the scholars, which the main idea is that according to the sparsity of the signal, the precise reconstruction of the sparse signal can be achieved by using the reconstruction algorithm through a small number of observations [17]–[20]. Authors in [17] proposed a new sparsity-aware framework to model and mitigate the joint effects of narrow-band interference (NBI) and IN in hybrid power line and unlicensed wireless communication systems. Authors in [18] adopted the classical CS-based greedy algorithm of sparsity adaptive matching pursuit (SAMP) to eliminate IN. Authors in [19] proposed the priori-aided SAMP (PA-SAMP) could effectively reconstruct IN with the aid of a priori partial support obtained from the proposed time-domain threshold, however, when the number of IN is large and the amount of transmitted data is large, the number of the priori partial support of the PA-SAMP algorithm is less. Authors in [20] proposed the optimized-prior-aided SAMP (OPA-SAMP) to solve this problem. OPA-SAMP could get the optimized threshold and the more accurate priori partial

support of IN, but it needs to know the power of IN and under the fixed INR (power ratio between background noise and impulse noise), which is hardly to achieve in practical applications. In order to improve the robustness and accuracy of the recovered IN, an improved-prior-aided SAMP (IPA-SAMP) was proposed in this paper, which could estimate the probability of IN, establish an improved prior aided support set of IN through the optimal threshold, reconstruct IN in time domain, and eliminate IN at the receiver. The main contribution of this paper is twofold:

1. Besides IN, the channel attenuation is another factor affecting the information interaction. Therefore, the PLC channel model between EVs and charging piles has been modeled, and the attenuation characteristics has been analyzed in this paper.

2. The traditional CS-based SAMP algorithm is significantly improved and the improved-prior-aided SAMP (IPA-SAMP) is proposed in this paper. The simulation results show that the reliability of information exchange system between EVs and charging piles based on IPA-SAMP-OFDM is significantly improved.

The rest of this paper is organized as follows. In section II, an information exchange system based on PLC between EVs and charging piles is proposed. The PLC channel model between EVs and charging piles is modeled in section III. In section IV, we model the noise model. The information interaction system based on CS-OFDM was modeled in section V. The simulated results of different methods to suppress IN under different signal-to-noise ratio (SNR) was provided in section VI. The conclusion and future work is presented in section VII.

Notation: $\|a\|_n$ represents the l_n norm operation of the vector a; $(A)^\dagger$ and $(A)^H$ denote the pseudo-inversion operation and conjugate transpose of the matrix A; A_Π represents the sub-matrix comprised of the Π columns of the matrix A; Π_c denotes the complementary set of Π; max(A,B) denotes the indices of the B largest entries of the vector A; $V|_\Pi$ denotes the entries of the vector V in the set of Π;

II. INFORMATION EXCHANGE SYSTEM MODEL BETWEEN EVS AND CHARGING PILES BASED ON PLC

The information exchange system between EVs and charging piles used the charging line as the PLC channel. Compared with the traditional methods of communication between EVs and charging piles, such as wireless and CAN communication, PLC between EVs and charging piles could simplify the charging interface and the charging line, reduce the cost and don't need the communication protocol conversion.

As shown in Fig. 1, the information exchange system between EVs and charging piles based on PLC mainly includes the BMS, sensors, vehicular electronic equipment and vehicular central electronic control unit (VCECU) in EVs' side, charging control unit (CCU) in charging piles' side. The VCECU is the core communication unit, which has the same function as a base station (BS) and is responsible for collecting all the data from terminal devices and sending the
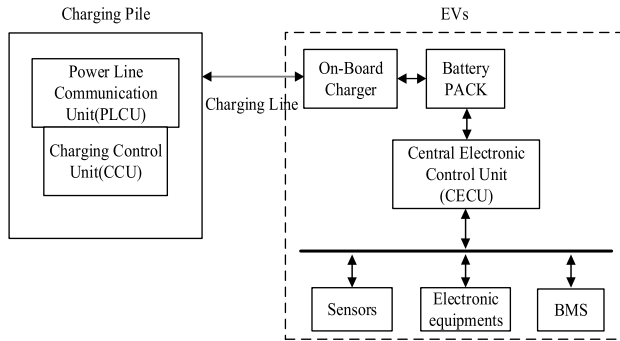
FIGURE 1. The information exchange system between EVs and charging piles based on PLC.

control command from VCECU to a specific terminal device such as BMS, sensors [5]. The charging line connected the on-border charger, after the power conversion, the battery is charged, the exchange of electric energy between EVs and charging piles is completed. The information exchange process between EVs and charging piles is described as follows, the VCECU collects the latest status information of EVs, and the status information will be send to the CCU via the charging line rather than the traditional communication line. The CCU could receive EVs status information and send the control command to EVs, which has realized information exchange between EVs and charging piles. The information received by CCU include the battery status information, the CCU could formulate the charging strategy to extend the battery life and could get a flexible charging and discharging strategy. In addition, the status information of EVs could be aggregated to the charging station via the communication line.

III. MODELING OF CHANNEL BETWEEN EVS AND CHARGING PILES

The charging power line is the medium for electric energy between EVs and charging piles, which is also the communication channel between EVs and charging piles. But the power line is not designed for the transmission of information, while designed for the transmission of electric energy. There is no consideration and design has been made for transmitting PLC signals [21]. There is no doubt that using the charging line as the PLC channel will cause signal attenuation. The attenuation of PLC signal between EVs and charging piles is mainly caused by the inherent impedance of the charging line channel and the impedance mismatch between the charging line and the battery impedance. The attenuation caused by the inherent impedance of the charging line channel is described in part A, and the impedance characteristics is introduced in part B.

A. ATTENUATION CHARACTERISTICS OF POWER LINE CHANNEL BETWEEN EVS AND CHARGING PILES

The transmission characteristics of the power line channel can be expressed by the characteristic impedance Z_0 and the

propagation constant γ.

$$Z_0 = \sqrt{(R_0 + j\omega L_0)/(G_0 + j\omega C_0)} \quad (1)$$
$$\gamma = \sqrt{(R_0 + j\omega L_0) \cdot (G_0 + j\omega C_0)} \quad (2)$$

When (2) is expanded by Taylor series and higher order items were omitted, (3) can be obtained.

$$\gamma \approx \frac{R_0}{2}\sqrt{\frac{C_0}{L_0}} + \frac{G_0}{2}\sqrt{\frac{L_0}{C_0}} + j\omega\sqrt{L_0 C_0} = \alpha(f) + j\beta \quad (3)$$

Among that, $\alpha(f)$ is the attenuation constant of the cable and β is the phase constant. $\alpha(f)$ and β can be expressed by C_0, L_0, R_0 and G_0, f is the carrier frequency of signal and $\omega = 2\pi f$ is the angular frequency.

The inherent attenuation of the PLC signal between EVs and charging piles is mainly caused by the inherent impedance of the charging line channel. The inherent attenuation of the charging line channel can be expressed in (4) [22].

$$H(f) = e^{-\alpha(f) \cdot l} \quad (4)$$

The attenuation degree of the cable is mainly determined by the length l and electrical parameters of the cable. The electrical parameters of the cable are closely related to the materials and specifications of the cable. The charging cable of EVs generally use copper core with tetraphenylethylene (TPE) insulated low-voltage power cable, with the insulation material is TPE and the conductor material is copper core. The cable section is shown in Fig.2.
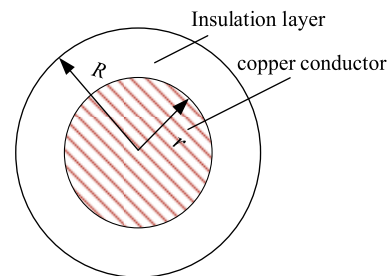

FIGURE 2. The cable section.

The cable with a conductor sectional area of 16 mm^2 is adopted in this paper, the nominal thickness of its insulation layer is usually 1 mm. The unit parameter can be obtained in (5) and (6).

$$R_0 = \frac{\rho}{\pi \cdot r^2} + \sqrt{\frac{f \cdot \rho \cdot \mu}{\pi \cdot r^2}} \quad (5)$$
$$C_0 = \frac{q}{u} = \frac{2\pi \cdot \varepsilon_0 \cdot \varepsilon_r}{In\frac{R}{r}} \quad (6)$$

ρ and μ are the resistivity and permeability of the copper conductor, r and R are the radius of conductor and cable, f is the carrier frequency, and ε_r is the dielectric constant of insulators, the dielectric constant of TPE is 2.35 and ε_0 is the vacuum dielectric constant.

B. THE IMPEDANCE CHARACTERISTICS

Impedance refers to the equivalent impedance of power line between the data transmitter and the data receiver, also known as input impedance, which mainly including the cable impedance and load impedance [23]. The impedance characteristic between EVs and charging piles mainly refers to the impedance characteristic of the battery on the side of EVs. The equivalent impedance circuit of the battery is shown in Fig. 3, and the simulated battery impedance is shown in Fig. 4 [24]. The parameters of the battery model is shown in Table 1.
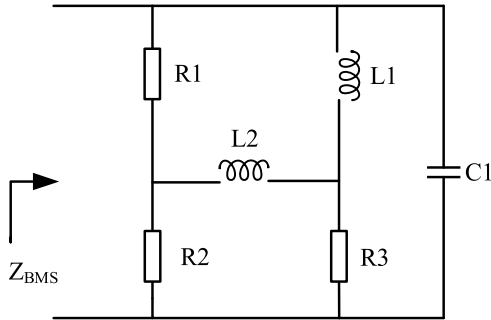
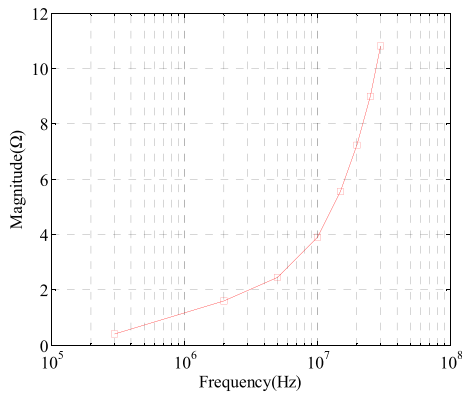**FIGURE 3.** The Equivalent circuit diagram of battery.

FIGURE 4. The impedance of the battery.

TABLE 1. The parameters of the battery.

R1	R2	R3	L1	L2	C1
2.5Ω	100MΩ	0.2Ω	180nH	80nH	10pF

The impedance of battery fluctuates with the change of the carrier frequency (from 300KHz to 30MHz), which results in the impedance mismatch between EVs and charging piles. The impedance mismatch would cause the reflection of the signal during the transmission, which affects the reliability of the communication.

When the impedance mismatch occurs, it will cause reflection of the transmitted signal. The reflection factor Γ_B and transmission factor T_B are shown in (7) and (8)

$$\Gamma_B = \frac{Z_L - Z_0}{Z_L + Z_0} \tag{7}$$

$$T_B = 1 - \Gamma_B \tag{8}$$

Z_L refers to the load impedance on the load side, Z_0 refers to the characteristic impedance of the communication line. The weight factor can be shown in (9).

$$g = 1 - \Gamma = T \tag{9}$$

C. CHANNEL TRANSFER FUNCTION MODELING

The transfer function of the channel can be modeled based on M. Zimmermann's and K. Dostert's theories [23], which using the "top-down" modeling method, its frequency and time domain calculations can be expressed in (10) and (11).

$$H(f) = g \cdot e^{-\alpha(f) \cdot l} \cdot e^{-j \cdot 2\pi f \left(\frac{l}{V_P}\right)} \tag{10}$$

$$H(t) = c \cdot \delta(t - \tau) \tag{11}$$

In (10), g denotes the weight factor of the transmission path, $e^{-\alpha(f) \cdot l}$ and $e^{-j2\pi \cdot f \cdot (l/V_p)}$ denote the attenuation and path delay of the transmission line. In (11), c represents the product of the weight factor of the channel and the inherent attenuation of the line, and τ is the time delay of the channel.

Considering the effects of impedance mismatch, inherent attenuation and delay, the attenuation of the PLC signal at a carrier frequency of 300 kHz to 30 MHz is shown in Figure 5.
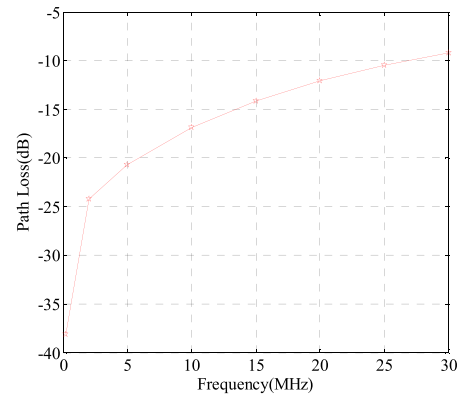
FIGURE 5. The channel attenuation between EVs and charging piles based on PLC.

It can be seen from Fig. 5 that the attenuation of the PLC signal decreases with the increase of the carrier frequency, which is mainly caused by impedance mismatch. When the carrier frequency is 30MHz, the attenuation is minimum. The carrier frequency with the least attenuation is selected in this paper.

IV. MODELING OF NOISE BETWEEN EVS AND CHARGING PILES

There are many electric devices, power electronic converter, sensor and relay in EVs and charging piles, when these electrical equipment works, noise will be generated, which will be injected into the PLC channel between EVs and charging piles. This can lead a serious channel environment and affect the efficiency of the information exchange, it is necessary to model the noise to verify the feasibility of PLC between EVs and charging piles. The noises in the channel between

EVs and charging piles mainly include two kinds of noise, background noise and IN.

Background noise has the most extensive impact on power line carrier communication, it can be expressed by Nakagami-m equation,

$$f(y) = \frac{(m/\Omega)^m}{\Gamma(m)} y^{2m-1} \exp(\frac{mr^2}{\Omega}) \quad (12)$$

y is a random variable, $\Omega = E(r^2)$ represents the average power of the background noise, $\Gamma(m) = \int_0^\infty x^{m-1} e^{-x} dx$ is Gamma function, $m = E^2(r^2)/var(r^2)$ is the "shape factor", which indicates the degree of relationship between the gaussian distribution and Rayleigh distribution. When $m = 1$, Nakagami-m obeys Rayleigh distribution, this means that noise can be regarded as white Gaussian noise. When the carrier communication frequency is high, m≈1, the background noise can be replaced by white Gaussian noise. The background noise between EVs and charging piles can be replaced by Gaussian noise with a mean value is 0.

IN between EVs and charging piles is mainly caused by the closure and open of power electronic devices, so the noise used in this paper is IN generated by the IGBT [26]. IN can be expressed by (13).

$$N(t) = A_m \sin(2\pi F_m t) e^{(-\frac{F_m}{\tau_m} t)} \quad (13)$$

A_m is the peak amplitude of IN, F_m is the pseudo-frequency, τ_m/F_m is the damping factor.

The parameters of IN model could be expressed by drawing the peak amplitudes and the pseudo frequencies from a normal distribution function whose means and variances are given in Table 2.

TABLE 2. The parameters of in.

State	Amplitude	Pseudo-Frequency (MHz)	τ_m
switch on	$N(2.61, 0.014)$	$N(4.3, 0.006)$	0.5
switch off	$N(0.09, 0.022)$	$N(0.46, 0.006)$	1

The IN model is built by the Matlab, the time domain figure and power spectral density figure of IN are obtained, as shown in Fig. 6 and Fig. 7.

As shown above, IN has strong periodicity with a period of $50\mu s$. The maximum amplitude of IN can reach 2.7. The power spectral density of IN increases significantly near 0.46MHz and 4.3MHz, and then concentrates around -80dBm/Hz. It can be seen that the impact of IN based on PLC between EVs and charging piles is more seriously.
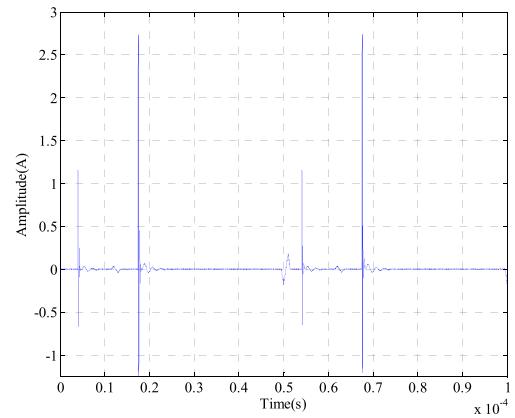

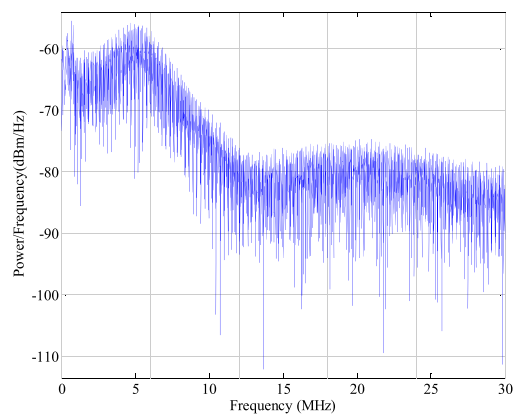**FIGURE 6.** Simulation of the IN in time domain.

FIGURE 7. Power spectral density of the IN.

V. MODELING THE INFORMATION INTERACTION SYSTEM BASED ON CS-OFDM

The communication environment of the channel between EVs and charging piles is seriously, the numerous IN injected to the channel have a larger amplitude, which seriously affects the reliability of communication system between EVs and charging piles. Therefore, in this paper, an improved-prior-aided sparsity adaptive matching pursuit (IPA-SAMP) which is used to remove IN has proposed in order to improve the reliability of the information exchange system between EVs and charging piles.

A. OFDM SYSTEM MODEL

OFDM technology is a multi-carrier modulation technology, which has high frequency efficiency and anti-frequency selective attenuation characteristics. The modulation and demodulation of OFDM can be realized by IDFT and DFT.

In the time domain, the length of the i-th OFDM data block $x_i = [x_{i,0}, x_{i,1}, \ldots, x_{i,N-1}]^T$ is N. The i-th time-domain OFDM data block is the IDFT of the associated frequency-domain data in the N sub-carriers. The channel impulsive response(CIR) for x_i is $h_i = [h_{i,0}, h_{i,1}, \ldots h_{i,N-1}]$, when the i-th OFDM data block pass the channel, y_i is received, $y_i = [y_{i,0}, \ldots, y_{i,N-1}] = h_i * x_i + u_i + w_i$, the

operator $*$ denotes circular convolution. Frequency domain signal Y_i can be obtained by DFT of the received signal y_i.

$$Y_i = F_N y_i = \text{diag}\{F_N h_i\} X_i + F_N u_i + F_N w_i \quad (14)$$

where F_N denotes the N-point DFT matrix. Let R is the set of the null sub-carriers, which is used for the recovery of IN. S_R is used to get the measurement vector p_i, it can be obtained from the null sub-carriers.

$$p_i = S_R Y_i = 0 + F_R u_i + F_R w_i \quad (15)$$

F_R is composed of the entries $\exp(-j2\pi mk/N)$, $k \in R$, $m = 0, \ldots, N - 1$. Where p_i is used for the recovery of IN. Compression sensing (CS) could be applied for the recovery of IN, it can be seen from (16) that the sparse IN u_i could be recovered from the measurement vector p_i. Reconstructing IN with unknown sparsity is equivalent to the convex optimization problem in (16).

$$\text{Min}\|u_i\|_1 \quad \text{s.t.}\|p_i - F_R u_i\|_2 \leq \delta \quad (16)$$

where δ is the *l2* of background noise in frequency domain. IN u_i can be reconstructed using the classical CS algorithm, but the sparsity of IN can not be directly obtained in PLC channels. In order to solve this problem, in this paper, we proposed the IPA-SAMP, which could select the optimal threshold to obtain the improved partial support, and then get the initial sparsity of IN. The acquisition of the improved IN partical support is described in part B. The IPA-SAMP is described in detail in the part C.

B. THE ACQUISITION OF THE IMPROVED IN PARTICAL SUPPORT

Unlike the previously PA-SAMP which get the partial support only according to the received signal, the proposed IPA-SAMP could further improves the accuracy of screening and the accuracy of the iterative process by the improved partial support.

The acquisition of the improved partial support such as the priori information could improve the accuracy of the CS algorithm and facilitate the recovery of IN.

The acquisition of the improved IN partial support is shown in Fig. 8. Firstly, we get the prior-aided IN partial support to count the probability of IN p. Secondly, we could get the optimized threshold according to the p, the signal power $P_{y_i'}$ and P_{x_i}. Lastly, we could get the improved IN partial support Π_i^1.

In the process of practical scene application, the probability of IN cannot be obtained directly in the actual channel, since the intensity of IN is obviously much higher than that of data component or background noise in the time domain, it is viable to obtain the probability of IN.

The indices of the time-domain samples in the i-th received OFDM data blocks with the average power exceeding the given threshold Γ_t are included in the partial support Π_i^0, which is given by,

$$\Pi_i^0 = \left\{ n \mid |y_{i,n}|^2 > \Gamma_t, n = 0, 1, \ldots, N - 1 \right\} \quad (17)$$

The power threshold of the received signal y_i is Γ_t, which is given by,

$$\Gamma_t = \lambda \cdot \frac{1}{N} \sum_{n=0}^{N-1} |y_{i,n}|^2, n = 0, 1, \ldots, N - 1 \quad (18)$$

where λ is a coefficient that can be configured large enough to ensure the accuracy of the prior-aided partial support Π_i^0. Let the probability of IN is p,

$$p = \frac{\|\Pi_i^0\|_0}{N} \quad (19)$$

The received i-th OFDM data block y_i would be attenuated after passing through the channel between EVs and charging piles. In order to ensure the accuracy of the recovered noise, the received i-th OFDM data block y_i is demodulated by DFT, after the channel equalized, the effect of the channel attenuation would be eliminated. Then, after IDFT modulation, the signal becomes y_i'. We could count the signal power $P_{y_i'}$, the transmission power P_{x_i} of the signal x_i are known, then we can count the sum power of IN and background noise P_{u+w}, while α is the attenuation coefficient of the channel,

$$\frac{P_{u+w}}{\alpha} = P_{y_i'} - P_{x_i} \quad (20)$$

The noise in the channel between EVs and charging piles is relatively serious, and the intensity of IN is higher than that of the background noise, ignoring the channel attenuation, $P_u \approx P_{y_i'} - P_{x_i}$. Then, the set of the improved IN partial support is stored in Π_i^1.

$$\Pi_i^1 = \left\{ n \mid |y_{i,n}'|^2 > \delta_t, n = 0, 1, \ldots, N - 1 \right\} \quad (21)$$
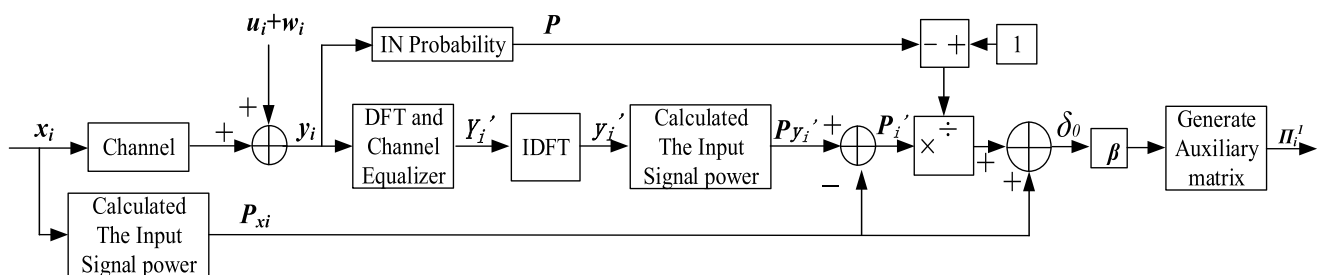

FIGURE 8. The algorithm flow diagram of the improved IN partial support Π_i^1.

TABLE 3. Parameters of the IPA-SAMP Algorithm 1.

Parameters(Input)	p_i	Π_i^1	$K_i^{(0)}$	$\Phi = F_R$
Implication	The measurement vector for the *i*-th OFDM data block with IN injected	Improved priori partial support of the *i*-th OFDM data block	Initial sparsity level of the *i*-th OFDM data with IN injected	Observation matrix
Parameters(Output)	u_i^k		Π_i^k	
Implication	The recovered IN injected into the *i*-th OFDM data block after the *k*-th iteration		The final partial support of IN injected into the *i*-th OFDM data block after the *k*-th iteration	

Π_i^1 is a collection of column number after screening; δ_t is the optimized threshold which is the product of constant value β and δ_0.

$$\delta_t = \beta \cdot \delta_0 = \beta \cdot \left(\frac{P_u}{(1-p)} + P_{x_i}\right) \quad (22)$$

In (22), P_{x_i} is the transmission power of the signal x_i, β is a constant in order to ensure the accuracy of the partial support.

C. IMPROVED CS-BASED ALGORITHM FOR IN RECOVER: IPA-SAMP

The improved IN partial support Π_i^1 could be obtain in the preceding content, with the aid of Π_i^1, we propose the IPA-SAMP algorithm whose pseudocode is summarized in Algorithm 1. The meaning of the input and output parameters we used in the Algorithm 1 is shown in Table 3.

The overall structure and explanations of each step of Algorithm 1 are described as follows.

Step 1, input. Input the improved priori partial support Π_i^1, sparsity level $K_i^{(0)} = \|\Pi_i^1\|_0$, the measurement vector p_i, and observation matrix $\Phi = F_R$, step size Δs to the IPA-SAMP algorithm.

Step 2, do the initialization. The initially recovered IN is set by $u_i^{(0)}|_{\Pi_i^1} \leftarrow \Phi^\dagger \cdot p_i$ and the initial testing sparsity level is set by $T \leftarrow \Delta s + K_i^{(0)}$.

Step 3, iterations. The iteration terminates until the halting condition (in line 17) is met. The iteration process includes the following. (*k* represents the number of the iterations)

(1) Preliminary test (Line 6), where the elements corresponding to the largest $T - K_i^{(0)}$ entries are generated by the residue matrix projection onto the dictionary $\Phi^H \cdot r^{(k-1)}$, is chosen as the preliminary list S_k.

(2) Make candidate list (Line 7), the candidate support list C_k for the current iteration is made by aggregating the preliminary test list S_k and the temporary final support of the previous iteration Π_i^k.

(3) Temporary final list (Line 8), where the temporary final support for the current iteration Π_t is established by selecting the largest T entries out of the projection of the

---

Algorithm 1 Improved Prior-Aided Sparsity Adaptive Matching (IPA-SAMP)

Input:
1. Π_i^1, 2. $K_i^{(0)} = \|\Pi_i^1\|_0$, 3. p_i, 4. $\Phi = F_R$, 5. Δs.

Initialization:
1. $K_i^{(0)} = \|\Pi_i^1\|_0$
2. $\Phi^\dagger \cdot p_i \rightarrow u_i^{(0)}|_{\Pi_i^1}$
3. $p_i - \Phi \cdot u_i^{(0)} \rightarrow r^{(0)}$
4. $\Delta s + K_i^{(0)} \rightarrow T, k \leftarrow 1, j \leftarrow 1$

Iterations:
5. do
6. $S_k \leftarrow \max(\Phi^H \cdot r^{(k-1)}, T - K_i^{(0)})$ {Preliminary test}
7. $C_k \leftarrow \Pi_i^k \cup S_k$ {Make candidate list}
8. $\Pi_t \leftarrow \max(\Phi_{C_k}^\dagger \cdot p_i, T)$ {Temporary final list}
9. $u_i^k|_{\Pi_t} \leftarrow \Phi_{\Pi_t}^\dagger \cdot p_i, u_i^k|_{\Pi_t^c} \leftarrow 0$
10. $r \leftarrow p_i - \Phi_{\Pi_t} \cdot \Phi_{\Pi_t}^\dagger \cdot p_i$ {Compute residue}
11. **if** $\|r\|_2 \geq \|r^{(k-1)}\|_2$ **then**
12. $T \leftarrow T + \Delta s$ {Stage switching}
13. **else**
14. $\Pi_i^{(k+1)} \leftarrow \Pi_t, r^{(k)} \leftarrow r$
15. $k \leftarrow k + 1$ {Same stage, next iteration}
16. **end if**
17. **while** $\|r\|_2 \leq \delta$
18. **Output:**
1. Support set Π_i^k
2. Recovered IN: $u_i^k|_{\Pi_i} \leftarrow F_{R_{\Pi_t}}^\dagger \cdot p_i, u_i^k|_{\Pi_i^c} \leftarrow 0$

---

measurements matrix p_i onto the plane spanned by the subset of the dictionary $\Phi_{C_k}^\dagger$ corresponding to the candidate list C_k.

(4) Compute residue (Line 9, Line 10), where the estimated IN matrix is calculated based on the least squares principle implemented on the temporary final support Π_t, and the residue matrix r is calculated using the estimated IN matrix.

(5) Stage switching (Line 11-Line16), when the l_2, 2-norm of the residue matrix is greater than that of the previous iteration, the stage would be switched and the testing sparsity

level T is increased by $\triangle s$, otherwise the stage keeps the same and the iteration goes into the next.

Step 4, output. The output of the algorithm includes the IN's final support set Π_i^k and the recovered IN.

The algorithm 1 above can accurately and efficiently recover IN u_i between EVs and charging piles. The time-domain signal y_i subtract the recovered IN u_i, then the signal is demodulated by OFDM and after the channel equalization then decoded to obtain the received data. Then the received data is compared with the original data to obtain the bit error rate (BER) of the information exchange system.

VI. SIMULATION ANALYSIS FOR THE COMMUNICATION SYSTEM BETWEEN EVS AND CHARGING PILES

The performance of the proposed IPA-SAMP algorithm for IN recovery and cancelation in the communication system between EVs and charging piles based on PLC is evaluated through simulations. The simulation parameters are as follows: the number of data sub-carriers is 128 and 256, the total number of sub-carriers is N = 1024, and the simulated SNR is from -10dB to 20dB, β is set to 2. The established channel model and IN are added in the simulation process. Since the noise between EVs and charging piles is much more complicated than the situation mentioned in this paper. Therefore, in the simulation, the period of IN changed from $50\mu s$ to $12.5\mu s$.

The reconstruction of IN in time domain when the data carrier is 128, and the SNR is 10 dB is shown in Fig. 9, the blue line and the red line represent thresholds for PA-SAMP and IPA-SAMP, respectively. According to the Fig. 9, the threshold value of IPA-SAMP proposed in this paper is significantly lower than the threshold value of PA-SAMP. Therefore, IPA-SAMP can select IN with a lower amplitude to expand IN support Π_i^1, which could improve the accuracy of the reconstructed IN.
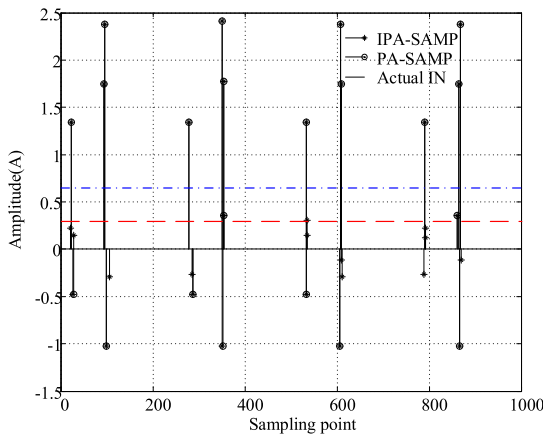

FIGURE 9. The reconstruction of IN in time domain when data carrier is 128, SNR is 10 dB.

The BER statistical results for OFDM, under the different IN mitigation methods and different SNR levels, with the number of the data sub-carrier is 256, is shown in

TABLE 4. The statistical result of BER under different in suppression methods when data carrier is 256.

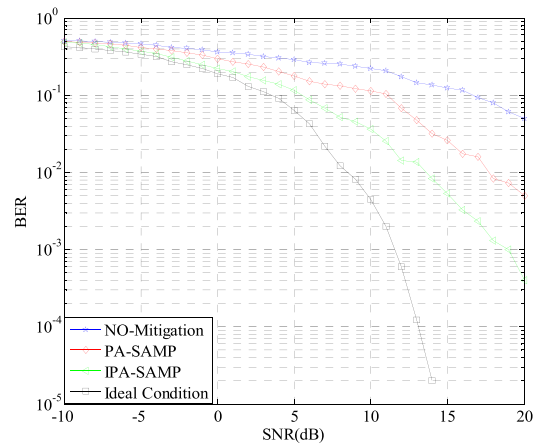|	BER			
SNR	NO MITIGATION	PA-SAMP	IPA-SAMP	IDEAL CONDITION
-10	0.51	0.4965	0.4843	0.42
-5	0.461	0.4138	0.3696	0.3412
-2	0.4039	0.3560	0.2763	0.25
0	0.3642	0.2933	0.2228	0.19
3	0.32029	0.2303	0.01625	0.11
7	0.2586	0.1401	0.0681	0.0216
10	0.2215	0.113	0.0366	0.0081
12	0.1748	0.0677	0.0144	0.002
14	0.1359	0.0317	0.0084	0.0001
16	0.1153	0.0176	0.0032	0
18	0.0802	0.0084	0.0013	0
20	0.05	0.005	0.0004	0

FIGURE 10. BER of the different IN suppression methods with the 256 data sub-carrier under the channel between EVs and charging piles.

Table 4 and Fig.10. The performance of the BER comparison could be more intuitive by Fig.10. The worst case is that there is no IN mitigation method is adopted and the channel attenuation is added, corresponding to the blue curve in Fig.10, even when the SNR is 20dB, the BER is still close to 0.05, which seriously affects the reliability of the information interaction between EVs and charging piles. The black curve in Fig. 10 corresponds to the ideal case that without the

interference of IN. Compared with the black curve and the blue cure in Fig. 10, it can be concluded that IN is the main factor affecting the reliability of the information interaction. The red curve in Fig.10 corresponds to the case that the PA-SAMP is adopted to suppress IN, compared with the blue curve, the BER has been reduced which means that IN has been suppressed to a certain extent. By comparing the case that the IPA-SAMP is adopted to mitigate IN, corresponding to the green curves in Fig. 10, it could be seen that the IPA-SAMP could suppress IN and reduce the BER significantly, which means that the IPA-SAMP proposed in this paper is obviously superior to the PA-SAMP.

When the number of the data sub-carrier changed from 256 to 128, the BER statistical results, under the different IN mitigation methods and different SNR levels is shown in Fig.11. The blue curve in Fig.11 is that there is no noise suppression algorithm is adopted. Due to the influence of channel attenuation and IN, even when the SNR is 20 dB, BER is about 0.01. The black curve in Fig. 11 corresponds to the case that add the channel attenuation but without the interference of IN. The red and green curves in Fig. 11 are BER curves when PA-SAMP and IPA-SAMP is adopted to suppress IN, respectively. The IPA-SAMP proposed in this paper is also obviously superior to the PA-SAMP when the data carrier is 128, but not as effective as the case that the data carrier is 256. Compared with the Fig. 10, we could concluded that when the number of data sub-carriers decreases, the BER of the four curves in Fig.11 decreases faster, which means that the communication reliability increases. The results show that the change of the number of data sub-carriers has more obvious effect on suppressing IN.
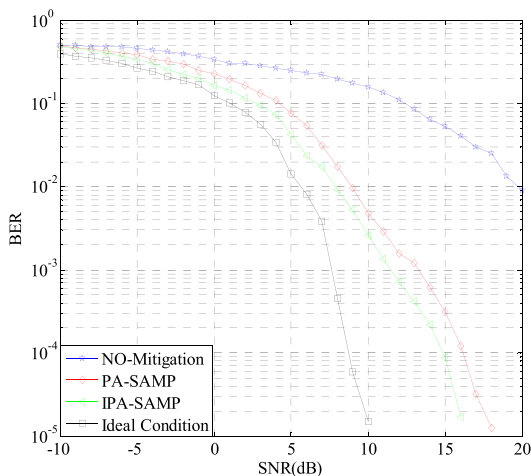

FIGURE 11. BER of the different IN suppression methods with the 128 data sub-carrier under the channel between EVs and charging piles.

VII. CONCLUSION AND FUTURE WORKS

Aiming at eliminating the influence of the IN, we proposed a novel IPA-SAMP IN cancelation scheme for OFDM-based information interaction system between EVs and charging piles in this paper. The proposed approach mainly includes

the following two steps: (1) the acquisition of the optimized threshold and the improved IN partial support; (2) with the help of the improved IN partial support, IN could be reconstructed by the proposed IPA-SAMP algorithm. At the receiver, we could eliminate the recovered IN. In order to get closer to the actual application scenario, in this paper, the channel model is modeled and added into the simulation process. Simulation results show that the IPA-SAMP algorithm improves the anti-interference ability and stability of the information interaction system between EVs and charging piles.

Future work can focus on improving the types of noise in the channel between EVs and charging piles, since the communication environment is more complicated than we mentioned in this paper, we need to add more typical noise. In addition, since this paper only study the communication reliability between EVs and charging piles, we intend to do the research on the communication performance within the charging station and the parking lot equipped with charging spots in future works.

REFERENCES

[1] J. Chen, Y. Zhang, and W. Su, "An anonymous authentication scheme for plug-in electric vehicles joining to charging/discharging station in vehicle-to-Grid (V2G) networks," *China Commun.*, vol. 12, no. 3, pp. 9–19, Mar. 2015.

[2] M. H. Amini, M. P. Moghaddam, and O. Karabasoglu, "Simultaneous allocation of electric vehicles' parking lots and distributed renewable resources in smart power distribution networks," *Sustain. Cities Soc.*, vol. 28, pp. 332–342, Jan. 2017.

[3] M. R. Mozafar, M. H. Amini, and M. H. Moradi, "Innovative appraisement of smart grid operation considering large-scale integration of electric vehicles enabling V2G and G2V systems," *Electr. Power Syst. Res.*, vol. 154, pp. 245–256, Jan. 2018.

[4] M. Nour, S. M. Said, A. Ali, and C. Farkas, "Smart charging of electric vehicles according to electricity price," in *Proc. ITCE*, Aswan, Egypt, 2019, pp. 432–437.

[5] L. Zhang, H. Ma, D. Shi, P. Wang, G. Cai, and X. Liu, "Reliability oriented modeling and analysis of vehicular power line communication for vehicle to grid (V2G) information exchange system," *IEEE Access*, vol. 5, pp. 12449–12457, 2017.

[6] P. Van Rensburg, H. Ferreira, and A. Snyders, "An experimental setup for in-circuit optimization of broadband automotive power-line communications," in *Proc. ISPLC*, Vancouver, BC, Canada, 2005, pp. 322–325.

[7] S. Barmada, M. Raugi, M. Tucci, and T. Zheng, "Power line communication in a full electric vehicle: Measurements, modelling and analysis," in *Proc. ISPLC*, Rio de Janeiro, Brazil, 2010, pp. 331–336.

[8] Y. Wang and J. S. Thompson, "Two–stage admission and scheduling mechanism for electric vehicle charging," *IEEE Trans. Smart Grid*, vol. 10, no. 3, pp. 2650–2660, May 2019.

[9] B. Sah, P. Kumar, R. Rayudu, S. K. Bose, and K. P. Inala, "Impact of sampling in the operation of vehicle to grid and its mitigation," *IEEE Trans. Ind. Informat.*, vol. 15, no. 7, pp. 3923–3933, Jul. 2019.

[10] R. M. Pratt and T. E. Carroll, "Vehicle charging infrastructure security," in *Proc. ICCE*, Las Vegas, NV, USA, Jan. 2019.

[11] X. Wu, Y. Dong, Y. Ge, and H. Zhao, "A high reliable communication technology in electric vehicle charging station," in *Proc. SSIRI-C*, Gaithersburg, MD, USA, 2013, pp. 198–203.

[12] S.-G. Yoon, S.-G. Kang, S. Jeong, and C. Nam, "Priority inversion prevention scheme for PLC vehicle-to-grid communications under the hidden station problem," *IEEE Trans. Smart Grid*, vol. 9, no. 6, pp. 5887–5896, Nov. 2018.

[13] J. Deng, C. Deng, C. Xie, and S. Quan, "Development of communication interface of AC charging for charging station based on ZigBee," in *Proc. CECNet*, XianNing, China, 2011, pp. 2130–2133.

[14] J. Rezgui, S. Cherkaoui, and D. Said, "A two-way communication scheme for vehicles charging control in the smart grid," in *Proc. IWCMC*, Limassol, Cyprus, Aug. 2012, pp. 883–888.

[15] S. Zhidkov, "Analysis and comparison of several simple impulsive noise mitigation schemes for OFDM receivers," *IEEE Trans. Commun.*, vol. 56, no. 1, pp. 5–9, Jan. 2008.

[16] S. Liu, F. Yang, X. Wang, J. Song, and Z. Han, "Structured-compressed-sensing-based impulsive noise cancelation for MIMO systems," *IEEE Trans. Veh. Technol.*, vol. 66, no. 8, pp. 6921–6931, Aug. 2017.

[17] M. Elgenedy, M. M. Awadin, R. Hamila, W. U. Bajwa, A. S. Ibrahim, and N. Al-Dhahir, "Sparsity–based joint NBI and impulse noise mitigation in hybrid PLC–wireless transmissions," *IEEE Access*, vol. 6, pp. 30280–30295, 2018.

[18] T. T. Do, L. Gan, N. Nguyen, and T. D. Tran, "Sparsity adaptive matching pursuit algorithm for practical compressed sensing," in *Proc. ACSSC*, Pacific Grove, CA, USA, Oct. 2019, pp. 581–587.

[19] S. Liu, F. Yang, W. Ding, and J. Song, "A priori aided compressive sensing approach for impulsive noise reconstruction," in *Proc. IWCMC*, Dubrovnik, Croatia, Aug. 2015, pp. 205–209.

[20] R. Deng, Z. W. Tan, G. X. Xiao, G. Wang, and H. L. Liu, "Impulse noise suppression in power line communication on compressed sensing," *Trans. China Electrotech. Soc.*, vol. 33, no. 23, pp. 5555–5563, Jun. 2018.

[21] W. B. Lu, H. Zhang, X. W. Zhao, and C. N. Suo, "The effect of network parameters for low-voltage broadband power line channels," *Trans. China Electrotech. Soc.*, vol. 31, no. S1, pp. 221–229, Dec. 2016.

[22] S. N. Li, X. R. Hu, K. Zheng, H. L. Sun, X. Z. Hou, and Y. Wang, "Measurement and research on attenuation characteristics of low voltage power line communication channel," *Power Syst. Protection Control*, vol. 46, no. 4, pp. 99–106, Feb. 2018.

[23] J. J. Qi, X. P. Chen, and X. S. Liu, "Advances of research on low voltage power line carrier communication technology," *Power Syst. Technol.*, vol. 34, no. 5, pp. 161–172, May 2010.

[24] A. P. Talie, W. A. Pribyl, and G. Hofer, "Electric vehicle battery management system using power line communication technique," in *Proc. PRIME*, Prague, Czech Republic, 2018, pp. 225–228.

[25] A. Chandra, A. Gupta, D. Mallick, and A. K. Mishra, "Performance of BFSK over a PLC channel corrupted with background Nakagami noise," in *Proc. ICCS*, Singapore, 2010, pp. 730–734.

[26] K. Kilani, V. Degardin, P. Laly, M. Lienard, and P. Degauque, "Impulsive noise generated by a pulse width modulation inverter: Modeling and impact on powerline communication," in *Proc. ISPLC*, Johannesburg, South Africa, 2013, pp. 75–79.

SHENGBIN CHI is currently pursuing the master's degree in electrical engineering with the Northeast Electric Power University, Jilin, China. His main interests and research field is the power line communication between the electric vehicles and the charging piles.

QUANGUI HU received the degree from Jiangxi University of finance and economics, in 2005. He is currently the Chief Engineer with the State Grid Information and Telecommunication Accenture Information Technology Company, Ltd., mainly focuses on grid information technology research, energy Internet advanced technology, and so on.

KANG CHEN is currently pursuing the master's degree in electrical engineering with Northeast Electric Power University, Jilin, China. His main interests and research field is energy Internet technology based on microgrid.

LIANG ZHANG received the B.Sc. degree from the Hebei University of Science and Technology, China, in 2007, and the M.S. and Ph.D. degrees in electrical engineering and automation from the Harbin Institute of Technology, Harbin, China, in 2010 and 2015, respectively. He was a Visiting Ph.D. Student with The University of British Columbia, Vancouver, BC, Canada, in 2014. He is currently an Associate Professor with the Department of Electrical Engineering, Northeast Electric Power University, China. His current research interests include ac/dc hybrid microgrids, V2G communication, vehicular communication, energy Internet, and power line communication.

LING LYU received the M.S. degree in control science and engineering from Yanshan University, Qinhuangdao, China. She is currently working as an Experimenter with Northeast Electric Power University, Jilin, China. Her main research fields are V2G and microgrid technology.

• • •